

CHAPTER 5

ANALYSIS OF EXTRAPOLATION VOLTAGES

In the previous chapters, the emphasis was on understanding the acoustical nonlinearities that would corrupt the ideal voltage based linear extrapolation. However, as was mentioned in Chapter 1, the spectrum of the drive voltage must also vary linearly as the drive amplitude is increased in order for linear extrapolation to be valid. Since no source is perfectly linear, it is impossible for the spectrum of the drive voltage to scale in a perfectly linear fashion. Furthermore, the amplitude of the drive voltage can be assessed by a variety of measures of the drive pulse. In the ideal linear case, all of the possible measures would result in equivalent extrapolation schemes. Unfortunately, since the source is not perfectly linear, some of the measures will yield more accurate results when used in the linear extrapolation.

In this chapter, six measures of the drive pulse are introduced as possible candidates for the extrapolation factor. Then, each is evaluated based on its ability to accurately perform linear extrapolation for all of the transducers and drive conditions considered in our experiment. Finally, a general extrapolation voltage is selected, and the extrapolation errors based on source nonlinearities for each transducer are predicted. These extrapolation errors will be used in the next chapter to quantify the uncertainties in our evaluation of the different nonlinear indicators.

5.1 Extrapolation Factor Candidates

The six different measures of the drive pulse considered in this thesis can be grouped into three distinct categories with each category contributing two possible extrapolation factors. The first category consisted of direct voltage measurements of the drive pulse. In this category, the two extrapolation factors that were considered were the

maximum amplitude voltage of the drive pulse, v_{op} , and the maximum peak-peak voltage of the drive pulse, v_{pp} , each of which was determined by

$$\begin{aligned} v_{op} &= \max_{t \in pulse} (|v(t)|) \\ v_{pp} &= \max_{t \in pulse} (v(t)) - \min_{t \in pulse} (v(t)) \end{aligned} \quad (5.1)$$

Clearly, the direct voltage measurements are the simplest measure of the drive pulse and are also the simplest linear extrapolation factors.

The next type of voltage measures considered were circuit-based measurements. In these measurements, the voltage pulse across the transducer was filtered analytically to try and capture the true spectrum being radiated by the transducer. In this way, our extrapolation would not be effected by circuit nonlinearities at frequencies outside of our range of interest. However, nonlinearities in frequencies radiated by the transducer would still corrupt our ability to perform linear extrapolation. The filtering approach is based on the idea that every piezoelectric transducer can be modeled as an equivalent RLC circuit shown in Figure 5.1 when excited near its fundamental resonant frequency [Bechmann and Fair, 1966].

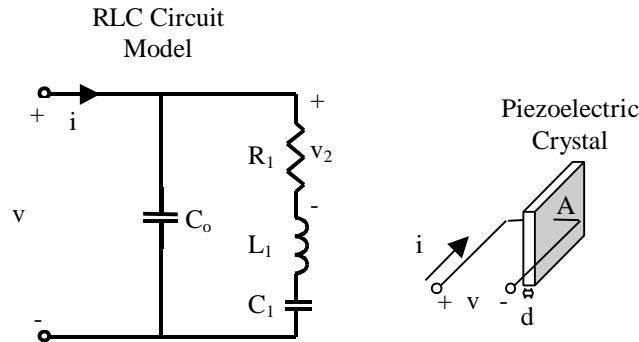


Figure 5.1: Equivalent RLC circuit model for a piezoelectric transducer.

In this circuit, the voltage v_2 across the resistor R_1 corresponds to the acoustical signal radiated by the piezoelectric crystal as well as other losses that might be present in the crystal. The reactive elements L_1 and C_1 capture the resonant behavior of the crystal. The capacitor C_o is the capacitance resulting from the fact that the transducer consists of a dielectric, the piezoelectric crystal, between two excited conducting surfaces as was discussed for the KLM model in Chapter 1 and Appendix B.

A comparison of the performance of the resistor-inductor-capacitor (RLC) circuit model to the KLM model is provided in Appendix D via numerical simulations. In the simulations, an air-backed lossless lithium niobate crystal with a crystal resonance of 5.5 MHz is evaluated by each of the models under different loading conditions. The different loading conditions were set by changing the characteristic impedance of the homogeneous region into which the crystal radiated. The most important results from this appendix are provided in Figure 5.2.

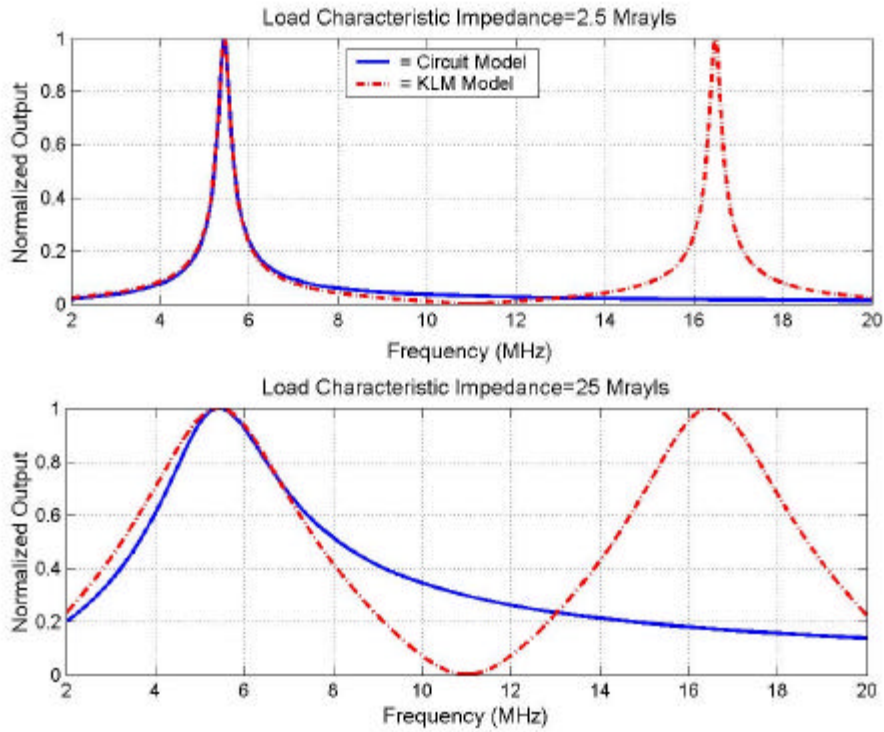


Figure 5.2: Comparison of output simulation results from the RLC circuit model and the KLM model under two different load conditions.

Notice that there is good agreement for small loading, 2.5 Mrayl, but the agreement degrades as the loading is increased, 25 Mrayl. Therefore, depending on the loading of the crystal in the transducer, the voltage across the resistor in the RLC circuit model should be close to the actual waveform generated by the transducer. However, our analysis did not include any frequency-dependent effects on the load impedance that would be introduced by the lens used to focus the acoustic waves, nor did it correctly portray the backing of the real transducers, which was a lossy, but matched, foam. A

more complete analysis of the RLC model considering these effects should be performed in the future if circuit-based extrapolation factors are selected as the standard, but such an analysis is beyond the scope of this preliminary work.

Before defining the circuit-based extrapolation factors considered in this thesis, the experimental procedure used to determine the circuit parameters for each transducer needs to be explained. *Bechmann and Fair* [1966] discuss the IEEE standard method for obtaining these values, however, their approach is only valid for high Q resonators. Since we had access to a HP network analyzer, we were able to determine the parameters from a full range of impedance measurements. The measurement was performed by connecting each transducer to the network analyzer through a 50- Ω transmission line. The transducer was then immersed in a beaker of water. The complex reflection coefficient S_{11} was then recorded and stored by the network analyzer over a range of frequencies about the fundamental resonant frequency for the transducer. The measured S_{11} values could then be analyzed by a computer to determine the values for the circuit parameters. The MATLAB code used to determine the parameters is provided in Appendix E. The range of frequencies over which the S_{11} values were measured for each transducer analyzed in this thesis is provided in Table 5.1.

The first step in calculating the circuit parameters from the data that was provided by the network analyzer was to translate the S_{11} values into admittance values at each frequency. This can be done by the equation [Pozar, 1998]

$$Y_{in} = Y_{line} \left(\frac{1 - S_{11}}{1 + S_{11}} \right) \quad (5.2)$$

where Y_{line} is the characteristic admittance of the transmission line connecting the load to the analyzer, which was 1/50 mho for our experiment. A plot illustrating a typical admittance curve for one of the transducers found using Equation (5.2) is shown in Figure 5.3. Theoretically, the input admittance for the transducer near the fundamental resonance should be given by

$$Y_{in_RLC} = j\omega C_o + \omega C_1 \frac{R_1 \omega C_1 - j(\omega^2 L_1 C_1 - 1)}{(R_1 \omega C_1)^2 + (\omega^2 L_1 C_1 - 1)^2} \quad (5.3)$$

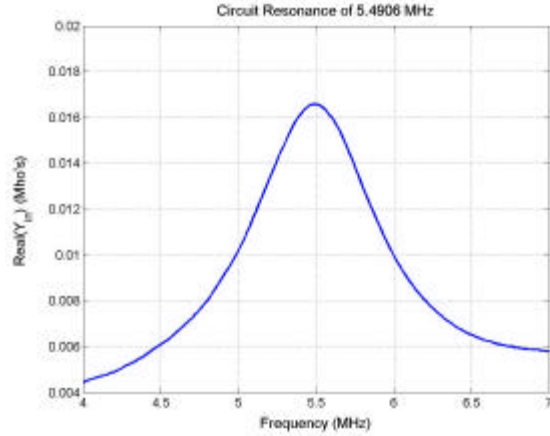


Figure 5.3: Example measured admittance curve for one of the transducers.

Therefore, once the values for the admittance had been determined for each frequency, a polynomial of degree 8 was used to fit the data very close to the resonant frequency. The range of frequencies used in the polynomial fit for each transducer is also provided in Table 5.1.

Table 5.1: Frequency ranges used to determine RLC parameters.

Transducer $f/\#$ (Diameter)	Circuit Resonant Frequency	Frequency Range of S_{11} Measurement (Step Size)	Frequency Range of Polynomial Fit to Admittance Data
1 (1.905 cm)	2.8072 MHz	2 MHz – 4.5 MHz (0.0125 MHz)	2.725 MHz – 2.900 MHz
1 (5.08 cm)	2.9983 MHz	2 MHz – 4.5 MHz (0.0125 MHz)	2.913 MHz – 3.088 MHz
1 (1.905 cm)	5.4906 MHz	4 MHz – 7 MHz (0.015 MHz)	5.395 MHz – 5.605 MHz
2 (1.905 cm)	5.3574 MHz	4 MHz – 7 MHz (0.015 MHz)	5.245 MHz – 5.455 MHz
1 (1.905 cm)	8.1517 MHz	7.2 MHz – 10 MHz (0.014 MHz)	8.040 MHz – 8.236 MHz

From this fit, the circuit resonant frequency, $\omega'_o = \frac{1}{\sqrt{L_1 C_1}}$, was determined by finding the frequency at which the real part of the fit admittance achieved a maximum

value. The admittance at this maximum value would also yield R_1 and C_o because $\text{Re}\{Y_{in}(\mathbf{w}'_o)\} = \frac{1}{R_1}$ and $\text{Im}\{Y_{in}(\mathbf{w}'_o)\} = \mathbf{w}'_o C_o$.

After performing the above analysis, the only quantities that need to be determined are the capacitance of C_1 and the inductance of L_1 . In order to do this, define a new parameter X_1 given by

$$\begin{aligned} X_1(\mathbf{w}) &= \text{Im}\left\{\frac{1}{Y_{in} - j\mathbf{w}C_o}\right\} \\ &= \text{Im}\left\{R_1 + \frac{j(\mathbf{w}^2 L_1 C_1 - 1)}{\mathbf{w}C_1}\right\} = \frac{\left(\left(\frac{\mathbf{w}}{\mathbf{w}'_o}\right)^2 - 1\right)}{\mathbf{w}C_1} \end{aligned} \quad (5.4)$$

Therefore, the value of C_1 should be given by

$$C_1 = \frac{\left(\left(\frac{\mathbf{w}}{\mathbf{w}'_o}\right)^2 - 1\right)}{\mathbf{w}X_1(\mathbf{w})} \quad (5.5)$$

for every value of \mathbf{w} . In our analysis, we determined the value of C_1 by solving Equation (5.6) for the range of X_1 values provided by our polynomial fit and taking the average. Once C_1 was known, L_1 could be determined from

$$L_1 = \frac{1}{\mathbf{w}'_o{}^2 C_1} \quad (5.6)$$

The circuit parameter values determined for each transducer are provided in Table 5.2.

Now that the values of the circuit parameters have been determined experimentally, extrapolation factors based on the RLC circuit model can be defined. Two possible extrapolation factors are the maximum amplitude voltage across R_1 v_{2op} and the maximum peak-peak voltage across R_1 v_{2pp} each of which can be determined from

$$\begin{aligned} v_{2op} &= \max_{t \in \text{pulse}} (|v_2(t)|) \\ v_{2pp} &= \max_{t \in \text{pulse}} (v_2(t)) - \min_{t \in \text{pulse}} (v_2(t)) \end{aligned} \quad (5.7)$$

where $v_2(t)$ is determined from

$$v_2(t) = \text{IFFT}\left\{V(\mathbf{w}) \frac{R_1 \mathbf{w} C_1}{R_1 \mathbf{w} C_1 + j(\mathbf{w}^2 L_1 C_1 - 1)}\right\} \quad (5.8)$$

Table 5.2: RLC parameters determined for each transducer.

Transducer $f/\#$ (Diameter)	Circuit Resonant Frequency	R_1	L_1	C_1	C_o
1 (1.905 cm)	2.8072 MHz	190.54 Ω	32.998 μH	97.408 pF	264.81 pF
1 (5.08 cm)	2.9983 MHz	30.983 Ω	8.3223 μH	338.58 pF	730.46 pF
1 (1.905 cm)	5.4906 MHz	60.320 Ω	7.2885 μH	115.28 pF	360.47 pF
2 (1.905 cm)	5.3574 MHz	46.161 Ω	9.2799 μH	95.103 pF	360.86 pF
1 (1.905 cm)	8.1517 MHz	33.752 Ω	3.1880 μH	119.57 pF	312.29 pF

In all four of the extrapolation factors defined previously, the factor was based on a time domain measure of the waveform. However, it is also possible to select factors in the frequency domain. One such factor is the magnitude of the drive waveform at the measured circuit resonance frequency for the transducer given by

$$V_{sn} = |V(\mathbf{w}'_o)| \quad (5.9)$$

This factor would directly relate to the pulse radiated by the transducer like the circuit-based factors discussed above; however, it would be less sensitive to errors in the values of the circuit parameters since the circuit resonant frequency is easy to determine experimentally. Another possible frequency domain extrapolation factor is the magnitude of the maximum frequency component across the simulated resistor R_1 :

$$V_{2,sn} = \max|V_2(\mathbf{w})| \quad (5.10)$$

This factor would be very similar to V_{sn} , however, it would have the advantage of increased sensitivity to the drive conditions. This increased sensitivity comes at the expense of a greater dependence on the measured circuit parameters.

5.2 Experimental Evaluation of Candidates

In the previous section, six different candidates for the extrapolation factor were introduced. In this section, each of these candidates will be evaluated experimentally. The evaluation was done by placing a PVDF membrane hydrophone (Marconi, Ltd., Essex, England) close to each transducer and recording the pressure waveforms for all of

the excitations used in the evaluation of the nonlinear indicators. The exact measurement procedure for obtaining these “close” waveforms will be discussed in Chapter 6 when the entire experimental procedure is described. For now, it is sufficient to know that the hydrophone was close enough to the transducer that nonlinear propagation effects could be ignored. Therefore, the candidates could be evaluated by determining which would yield the best performance when used to linearly extrapolate the “close” waveforms.

Before the proposed extrapolation factors can be evaluated, it is critical to confirm that the “close” pressure waveforms vary in a linear fashion. If they do not vary linearly, then we cannot expect any of the factors to give good extrapolation results. The linearity of the “close” pressure waveforms can be evaluated by first selecting some reference waveform from the current set of measurements being evaluated. Then, the peak compressional pressure p_c of the reference waveform can be linearly extrapolated and compared to the values for the other waveforms using the peak rarefactional pressure p_r as the extrapolating factor for each waveform. If the variation in the waveforms is perfectly linear, the extrapolated and measured p_c values should be identical. By calculating the error between the extrapolated and measured values, it is possible to quantify the linearity of the “close” waveforms. Of course, it would also be possible to perform the evaluation using p_c as the extrapolation factor and comparing the errors in the p_r values.

The formula used to calculate the errors between the extrapolated and measured p_c values using the rarefactional pressure, p_r , as the extrapolation factor was

$$\%Error_{-p_c}(p_r) = 100 \cdot \left| 1 - \frac{p_c - ref}{p_c} \frac{p_r}{p_r - ref} \right| \quad (5.11)$$

where $_{-ref}$ refers to the value of the quantity for the reference waveform. A typical error curve for one of the transducers calculated using this formula is provided in Figure 5.4. This particular curve corresponds to the $f/\#1$ transducer with a circuit resonant frequency of 5.4906 MHz excited by a “three cycle” “positive going” pulse (3p). The “three cycle” “positive going” excitation condition will be explained in Chapter 6.

Notice that in Figure 5.4, the error exhibits a sharp rise at low and high voltage settings. The rise at high voltage settings corresponds to a physical change in the

waveform. However, the rise at low voltage settings is due to quantization effects in the digital oscilloscope used to acquire the “close” pressure waveforms.

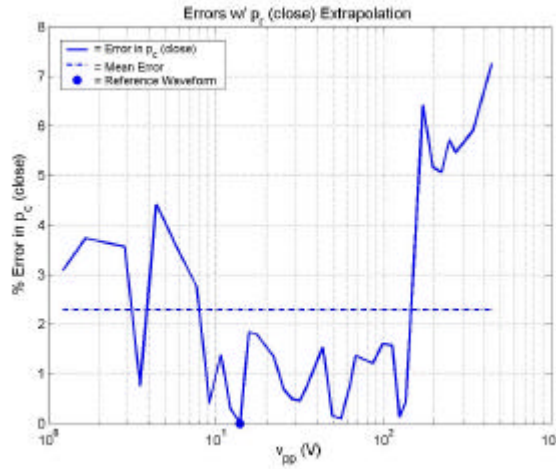


Figure 5.4: Typical errors in p_c using p_r as an extrapolation factor.

Since these errors were not a reflection on the true linearity of the waveform, they were excluded when the linearity was quantified. This was done by selecting the reference waveform to be the waveform with the smallest amplitude such that the quantization error given by

$$\%Error_Quantization = 100 \left(\frac{V_{step}}{Cal_{factor} p_c} \right) \quad (5.12)$$

was less than 2% where V_{step} is the smallest quantization step size for the digital oscilloscope (62.5 μ V) and Cal_{factor} is the calibration factor for the hydrophone (42.5 mV/MPa). The linearity of the “close” pressure waveforms was then quantified by finding the mean error of Equation (5.11) for all excitations with larger v_{pp} than the reference waveform for each data set. The MATLAB code used to perform this analysis is provided in Appendix F.

The mean errors in the “close” pressure waveforms for each data set considered in the experiment are given in Table 5.3. Clearly, for all experiments, the scaling of the “close” pressure values was sufficiently linear so that the data could be used to evaluate voltage based linear extrapolation. The “Drive Pulse” column in Table 5.3 refers to the properties of the drive pulse selected for our pulse generator. The number (i.e., 1 or 3) refers to the selected number of cycles in the drive pulse, and the letter (p or n) refers to

whether the first peak of the voltage pulse was at a positive or a negative voltage (i.e., positive or negative going). More is said about these drive conditions in Chapter 6.

Table 5.3: Linearity of the “close” pressure waveforms quantified in terms of the mean extrapolation error using p_r as the extrapolation factor.

Transducer $f/\#$ (Diameter)	Resonant Frequency	Drive Pulse # of Cycles, \pm Going	%Error in p_{close}
1 (1.905 cm)	2.8073 MHz	3, p	1.4801
1 (5.08 cm)	2.9983 MHz	3, p	0.6952
1 (1.905 cm)	5.4906 MHz	1, p	1.9756
1 (1.905 cm)	5.4906 MHz	3, p	2.2844
1 (1.905 cm)	5.4906 MHz	3, n	2.7193
2 (1.905 cm)	5.3574 MHz	3, p	1.8603
1 (1.905 cm)	8.1517 MHz	3, p	4.1700

At this point, the different candidates for the extrapolation factor can be evaluated for each of the transducers and drive conditions considered in the experiment. The evaluation will be performed in much the same way as the linearity of the “close” waveforms were evaluated. First, the extrapolation error will be calculated for each measurement in a particular data set using equations of the form

$$\%Error_{-p_{c,r,avg}}(Factor) = 100 \cdot \left| \frac{p_{c,r,avg} - (p_{c,r,avg} - ref) \frac{Factor}{Factor_{ref}}}{p_{c,r,avg}} \right| \quad (5.13)$$

In this equation, $Factor$ represents the current extrapolation factor being evaluated, $_{ref}$ refers to the value of the quantity for the reference waveform, and the subscript c,r,avg references the peak compressional p_c , peak rarefractional p_r , and peak average $p_{avg} = (p_c + p_r)/2$, pressures, respectively, for the “close” waveforms. The reason for evaluating the p_c , p_r , and p_{avg} errors independently will be clear in Section 5.3.

After determining the extrapolation errors for a particular candidate, quantization effects will be removed, and the error will be quantified by finding its mean as was done when evaluating the linearity of the “close” pressure waveforms. Since the quantization errors of the “close” waveform would be the same as in the linearity analysis, the same reference value can be selected. Furthermore, the error can be quantized by finding the mean error for all voltage settings greater than the reference setting as was done in the

previous analysis. The MATLAB code used to perform the calculations is found in Appendix F. The mean extrapolation errors using each of the candidates defined in Section 5.1 for each transducer and drive condition are provided in Tables 5.4, 5.5, and 5.6.

Table 5.4: Evaluation of extrapolation factors for p_c quantified in terms of the mean extrapolation error determined from the “close” pressure waveforms.

Transducer $f/\#$ (Diameter)	Resonant Frequency	Drive Pulse	%Error w/ v_{op}	%Error w/ v_{pp}	%Error w/ v_{2op}	%Error w/ v_{2pp}	%Error w/ V_{sn}	%Error w/ V_{2sn}
1 (1.905 cm)	2.8073 MHz	3, p	<u>1.9321</u>	2.3122	<u>2.7938</u>	<u>2.8148</u>	2.6165	2.5452
1 (5.08 cm)	2.9983 MHz	3, p	1.2780	<u>1.5731</u>	1.4278	1.4434	<u>1.4611</u>	<u>1.2016</u>
1 (1.905 cm)	5.4906 MHz	1, p	2.6685	<u>2.1198</u>	2.6296	2.8912	<u>5.1901</u>	<u>4.0512</u>
1 (1.905 cm)	5.4906 MHz	3, p	1.9231	1.9589	2.0452	<u>2.0679</u>	<u>2.0664</u>	<u>1.8698</u>
1 (1.905 cm)	5.4906 MHz	3, n	<u>3.7192</u>	3.2766	3.3848	3.4053	<u>3.4157</u>	<u>3.2092</u>
2 (1.905 cm)	5.3574 MHz	3, p	3.1599	<u>3.3737</u>	2.9659	3.0189	<u>3.3422</u>	<u>2.9462</u>
1 (1.905 cm)	8.1517 MHz	3, p	<u>5.1317</u>	5.0493	<u>5.3202</u>	4.9882	<u>4.8995</u>	5.0125
MEAN ERROR VALUES			2.8304	<u>2.8091</u>	2.9382	2.9471	<u>3.2845</u>	<u>2.9765</u>

Table 5.5: Evaluation of extrapolation factors for p_r quantified in terms of the mean extrapolation error determined from the “close” pressure waveforms.

Transducer $f/\#$ (Diameter)	Resonant Frequency	Drive Pulse	%Error w/ v_{op}	%Error w/ v_{pp}	%Error w/ v_{2op}	%Error w/ v_{2pp}	%Error w/ V_{sn}	%Error w/ V_{2sn}
1 (1.905 cm)	2.8073 MHz	3, p	<u>1.1353</u>	1.5850	<u>1.8411</u>	<u>1.8582</u>	1.6551	<u>1.5817</u>
1 (5.08 cm)	2.9983 MHz	3, p	<u>1.1032</u>	<u>1.6802</u>	1.4926	1.5198	<u>1.5356</u>	<u>1.2729</u>
1 (1.905 cm)	5.4906 MHz	1, p	2.5204	1.9883	<u>1.8468</u>	<u>1.5908</u>	<u>3.8527</u>	<u>2.6458</u>
1 (1.905 cm)	5.4906 MHz	3, p	<u>2.1799</u>	<u>1.7649</u>	<u>1.6053</u>	<u>1.5866</u>	1.7607	<u>1.6726</u>
1 (1.905 cm)	5.4906 MHz	3, n	<u>2.4061</u>	<u>1.8511</u>	1.5291	<u>1.4838</u>	1.7224	<u>1.5191</u>
2 (1.905 cm)	5.3574 MHz	3, p	<u>1.8497</u>	1.7832	<u>1.5640</u>	<u>1.5648</u>	<u>2.0237</u>	1.7905
1 (1.905 cm)	8.1517 MHz	3, p	<u>1.6055</u>	<u>1.2177</u>	<u>1.6235</u>	<u>1.2390</u>	1.2465	1.3139
MEAN ERROR VALUES			1.8286	1.6958	<u>1.6432</u>	<u>1.549</u>	<u>1.971</u>	1.6852

Table 5.6: Evaluation of extrapolation factors for p_{avg} quantified in terms of the mean extrapolation error determined from the “close” pressure waveforms.

Transducer $f/\#$ (Diameter)	Resonant Frequency	Drive Pulse	%Error w/ v_{op}	%Error w/ v_{pp}	%Error w/ v_{2op}	%Error w/ v_{2pp}	%Error w/ V_{sn}	%Error w/ V_{2sn}
1 (1.905 cm)	2.8073 MHz	3, p	<u>1.3440</u>	<u>1.8013</u>	<u>2.3185</u>	<u>2.3350</u>	2.1324	2.0595
1 (5.08 cm)	2.9983 MHz	3, p	<u>1.1458</u>	<u>1.6110</u>	1.4574	1.4755	<u>1.4842</u>	<u>1.2881</u>
1 (1.905 cm)	5.4906 MHz	1, p	2.3795	<u>1.8148</u>	<u>1.9931</u>	2.2160	<u>4.5662</u>	<u>3.3877</u>
1 (1.905 cm)	5.4906 MHz	3, p	<u>1.5890</u>	1.3266	1.2178	<u>1.2157</u>	<u>1.3533</u>	<u>1.2172</u>
1 (1.905 cm)	5.4906 MHz	3, n	<u>2.7231</u>	<u>2.1280</u>	2.2470	<u>2.2758</u>	2.2757	<u>2.1089</u>
2 (1.905 cm)	5.3574 MHz	3, p	2.3365	<u>2.5001</u>	<u>2.1732</u>	2.2077	<u>2.4623</u>	<u>2.1311</u>
1 (1.905 cm)	8.1517 MHz	3, p	<u>3.2281</u>	3.1744	<u>3.5085</u>	3.0976	<u>3.0556</u>	3.2124
MEAN ERROR VALUES			2.1066	<u>2.0509</u>	2.1308	2.1176	<u>2.4757</u>	<u>2.2007</u>

Notice that from the result presented in the above tables, all of the error values are on the order of 2%-5%, and all are approximately the same. This means that our system is sufficiently linear that any one of the candidates could be selected for the extrapolation voltage. Unfortunately, this also makes it difficult to narrow the search to make the final selection. In order to facilitate a comparison, the maximum and minimum values for each row in the table have been emphasized in bold print. Furthermore, the maximum values have been underlined and the minimum values have been italicized. Also, the second minimum values have been italicized and the second maximum values are underlined, but neither of these values are printed in bold. Although it would be possible to select an extrapolation factor for each of p_c , p_r , and p_{avg} , we shall simplify our later analysis by only choosing one extrapolation factor.

Notice for all three pressure extrapolations, V_{sn} gives the largest mean error. Therefore, V_{sn} is probably not the best choice for the extrapolation factor. However, the differences in the errors between the other factors are small. In order to make a choice, a scoring scheme was implemented where each minimum value was worth 2 points, each second minimum 1 point, each maximum -2 points, and each second maximum -1 point. The scoring scheme was selected in order to emphasize the performance of each factor within the individual data set. Referring back to Figure 5.4, notice that there is a sudden jump in the error at high voltage settings. Most of the transducers exhibited this jump; however, the location and duration of the jump varied for each data set. Therefore, the mean error values between the data sets would be affected. However, within a data set, the statistics would be the same for each extrapolation factor being considered. For this same reason, the last row in each table containing the mean error values was excluded from the scoring scheme. The score for each of the candidates is shown in Table 5.7. Based on this scheme, V_{2sn} had the highest score and hence was selected as the extrapolation factor for my experiments. Recall that V_{2sn} was the voltage at the maximum frequency component across the simulated resistor R_1 . However, a more rigorous analysis could result in a different factor yielding the best performance, but our analysis is sufficient for this study.

Table 5.7: Scores used to select the best extrapolation factor.

Extrapolation Candidate	Score for p_c	Score for p_r	Score for p_{avg}	Total Score
v_{op}	+1	-2	-1	-2
v_{pp}	0	-2	0	-2
v_{2op}	-1	+1	-1	-1
v_{2pp}	-3	+6	0	+3
V_{sn}	-4	-5	-3	-12
V_{2sn}	+7	+2	+5	+14

5.3 Setting the Confidence Measure for Each Data Set

Before concluding our discussion of the extrapolation factors, we can also use the information gleaned from our experimental evaluation of the different candidates to set a confidence measure for use in our experimental evaluation of the nonlinear indicators. Recall that the goal of this thesis is to determine an indicator of nonlinearity that could be used to set the range of drive voltages over which linear extrapolation of the pressure values at the focus could be performed. However, any nonlinearities that occur prior to the acoustic wave entering the propagating medium, water, would introduce uncertainties in our evaluation. Fortunately, the effect of all of these nonlinearities has already been quantified by our evaluation of the different possible extrapolation factors.

In the previous section, the errors in linear extrapolation for each of the proposed extrapolation factors were evaluated by finding the mean error in the extrapolation for each candidate. In Chapter 7, the linearity of the waveform at the focus under each drive condition for a particular transducer will be evaluated by determining when a polynomial fit to the extrapolation error exceeds some acceptable level. Since only the mean errors would significantly alter the outcome of the polynomial fit, the uncertainties introduced by nonlinearities prior to the acoustic wave entering the medium would be adequately quantified by the error values provided in Tables 5.4, 5.5, and 5.6. Therefore, for each data set, the appropriate error factor can be selected from column 6, V_{2sn} , in Table 5.4, 5.5, or 5.6 corresponding to whether linear extrapolation is being evaluated for p_c , p_r , or p_{avg} . More will be said on how these error values are incorporated into the evaluation of the nonlinear indicators in Chapter 7.